

# Supporting Information

## Effective upgrade of levulinic acid into $\gamma$ -valerolactone over an inexpensive and magnetic catalyst derived from hydrotalcite precursor

Jun Zhang,<sup>†</sup> Jinzhu Chen,<sup>\*,†</sup> Yuanyuan Guo,<sup>†</sup> and Limin Chen<sup>‡</sup>

<sup>†</sup>*CAS Key Laboratory of Renewable Energy, Guangzhou Institute of Energy Conversion, Chinese Academy of Sciences, Guangzhou 510640, P.R. China*

<sup>‡</sup>*School of Environment and Energy, South China University of Technology, Guangzhou Higher Education Mega Centre, Guangzhou 510006, P.R. China*

*\*Corresponding author. Tel./Fax: (+86)-20-3722-3380. E-mail address: [chenjz@ms.giec.ac.cn](mailto:chenjz@ms.giec.ac.cn)*

## Materials

LA (99%), 2-methyltetrahydrofuran (MTHF, 99.5%), GVL (98%), Ru/C (Ru loading: 5%), Pd/C (Pd loading: 5%) and Pt/C (Pt loading: 5%) were purchased from Aladdin Reagent Co. Ltd. (Shanghai, China). Methyl levulinate (ML) were provided by Alfa Aesar Co. Ltd. (Tianjin, China). All other chemicals were supplied by Lingfeng Chemical Reagent Co. Ltd. (Shanghai, China) and used without further purification.

## Catalysts preparation

The HTICs with different Ni:Cu:Al:Fe atomic ratios were synthesized by the co-precipitation method described earlier.<sup>1</sup> Two aqueous solutions, one containing a mixture of metal nitrates and the other precipitating agent (NaOH and Na<sub>2</sub>CO<sub>3</sub>), were added slowly while the pH was maintained between 9 and 10. The resulting suspension was aged at 333 K for 8 h. The precipitate was washed with distilled water until the pH value of the filtrate was around 7 and then dried at 353 K for 24 h. Mg, Zn and Co modified Ni/Cu/Al/Fe hydrotalcite compounds were prepared according to the above method with the addition of corresponding metal nitrates. The precipitate was ground to fine powders and then activated at 773 K for 3 h in a H<sub>2</sub> atmosphere prior to the experiment.

## Catalyst characterization

Chemical analyses were measured by a Thermo Elemental ICP-AES spectrometer after dissolution of the samples in a HNO<sub>3</sub> solution. Powder X-ray powder diffraction (XRD) was performed on a Bruker D8 Advance diffractometer using Cu K $\alpha$  radiation generated at 40 kV and 40 mA. X-ray photoelectron spectroscopy (XPS) measurements were made on a Kratos Ultra system employing an Al K $\alpha$  radiation source. The binding energies for each spectrum were calibrated with a C1s spectrum of 284.6 eV. High-resolution spectra of Ni 2p and Cu 2p were recorded at pass energy of 40 eV and resolution of 0.1 eV per step, for quantitative measurements of binding energy.

The Brunauer-Emmett-Teller (BET) surface area measurements were performed with N<sub>2</sub> adsorption-desorption isotherms at 77 K (SI-MP-10, Quantachrome). Before test, the samples were degassed under vacuum at 473 K for 16 h. The morphological analysis for recycled catalysts was carried out using high resolution transmission electron microscopy (HR-TEM, JEM-2100HR). For sample preparation, a small amount of catalysts were firstly dispersed in ethanol solution, and then a drop of the suspension was placed onto copper grid, followed by evaporating the solvent.

The measurements of catalyst acidity were carried out on a Micromeritics AutochemII 2920 chemisorption analyzer following an ammonia temperature-programmed desorption (TPD) method. For each run, the sample was heated up to 873 K at a rate of 20 K min<sup>-1</sup> and kept for 0.5 h in a He flow to remove adsorbed impurities. Then the sample was cooled down to 373 K for the adsorption of NH<sub>3</sub>. After flushing with He for 1 h to remove physically adsorbed NH<sub>3</sub>, the TPD data were collected from 373 K to 1073 K with a ramp of 20 K min<sup>-1</sup>.

Py-IR analysis was conducted on Bruker FT-IR Tensor 27 equipped with BX-5 in situ transmission FT-IR device, to identify acid type and concentration of prepared catalyst. About 20 mg sample was pressed into a self-supporting disk of 13 mm diameter, and was placed in a quartz cell

connected to a conventional closed gas-circulation system. The sample disk was pretreated at 473 K for 2 h in a pressure of  $1.0 \times 10^{-3}$  Pa and then the temperature was cooled to 313 K for collecting single channel background spectrum. For adsorption experiment, pyridine was introduced to the sample for 20 min. IR spectra were measured at 313 K after adsorption balance, followed by evacuation to remove adsorbed pyridine for collecting IR spectra at 423 K (heating rate,  $10 \text{ K min}^{-1}$ ) and 673 K (heating rate,  $10 \text{ K min}^{-1}$ ).

### Products analysis

The quantity of liquid samples in organic phase was analyzed by Agilent 6890 equipped with a flame ionization detector (FID) and a KB-5 capillary column ( $30.0 \text{ m} \times 0.32 \text{ } \mu\text{m} \times 0.25 \text{ } \mu\text{m}$ ) using nitrogen as the carry gas. The GC-MS analysis was recorded on Trace GC-MS 2000, equipped with a 30 m HP-5 (0.25 mm internal diameter). The operating conditions for GC and GC-MS were as follows: injector port temperature, 533 K; column temperature, initial temperature 323 K (2 min), gradient rate  $30 \text{ K min}^{-1}$ , final temperature 503 K (1 min), flow Rate  $75 \text{ mL min}^{-1}$ .

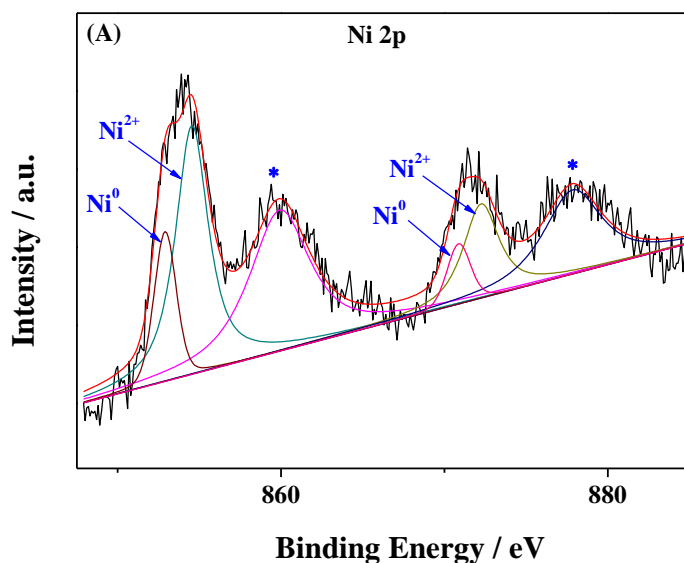
The HPLC analysis of final products in aqueous phase was performed on Shimadzu LC-20AT equipped with an UV/refractive index detector and a Shodex Sugar SH-1011 column ( $\varnothing 8 \times 300 \text{ mm}$ ).  $0.005 \text{ M H}_2\text{SO}_4$  was used as the mobile phase at a flow rate of  $0.5 \text{ mL min}^{-1}$ , and the column temperature was 323 K.

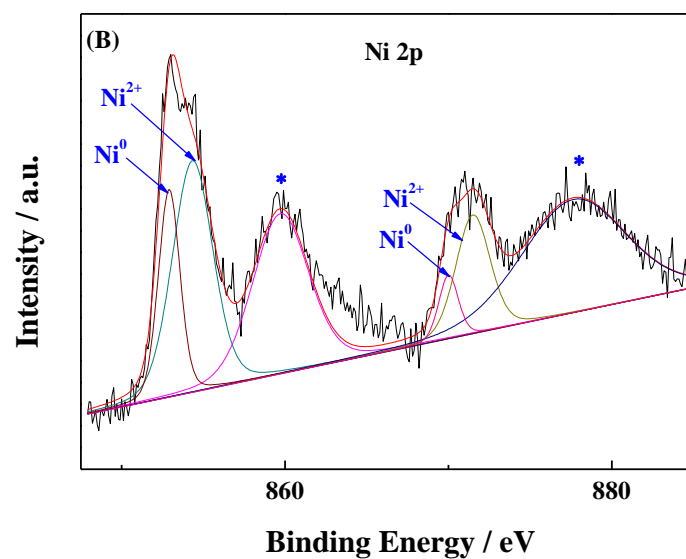
The corresponding formulas for calculating GVL selectivity and turnover frequency (TOF value) were defined below:

$$\text{GVL selectivity} = [\text{GVL yield} / \text{LA conversion}] \times 100\%$$

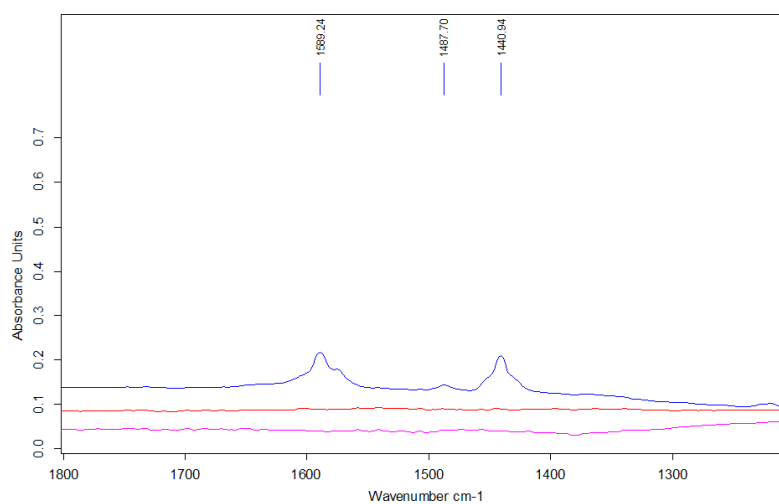
$$\text{TOF} = m_{\text{GVL}} / (m_{(\text{Ni}+\text{Cu})} \times t)$$

And where  $m_{\text{GVL}}$ ,  $m_{(\text{Ni}+\text{Cu})}$ , and  $t$  stand for the moles of GVL produced, the total moles of Ni and Cu used, and the reaction time.

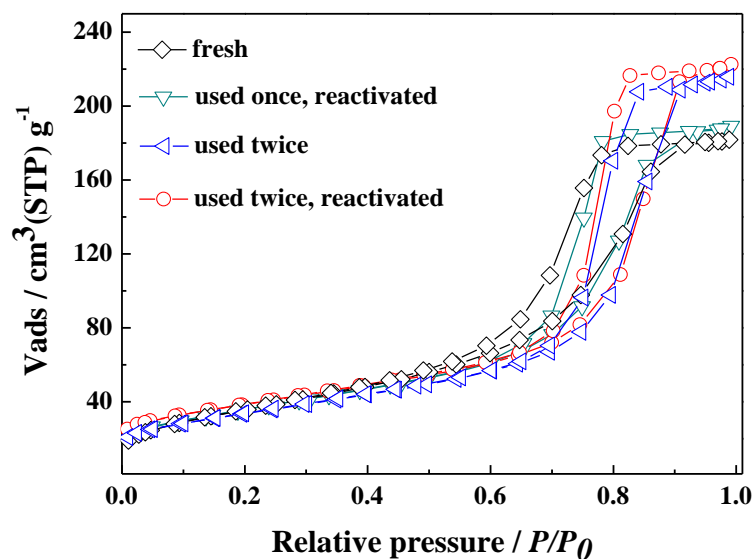




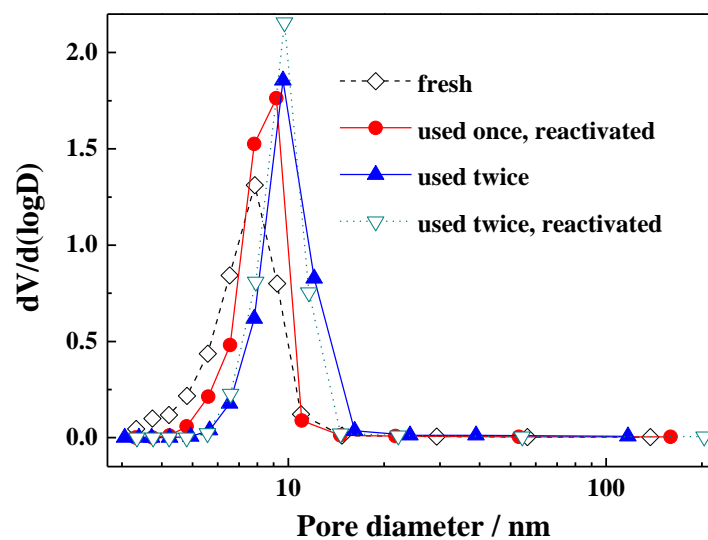
**Figure S1** XPS spectra of Ni 2p for reduced M8 catalyst: (A) 623 K; (B) 773 K.



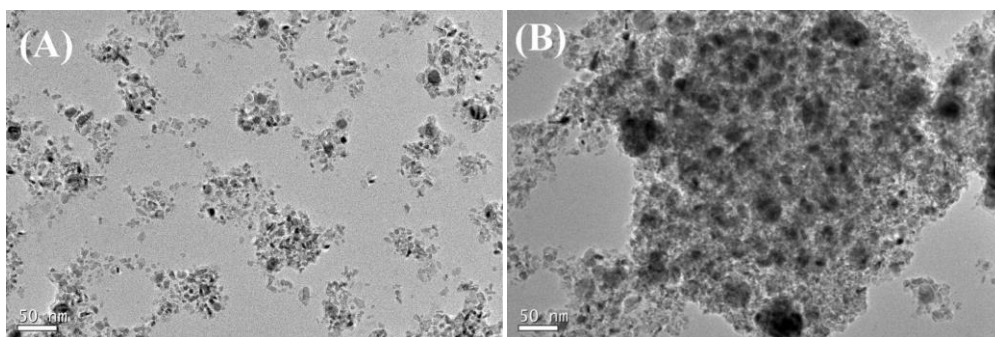
**Figure S2** IR spectrum of pyridine adsorbed on magnetic M5 catalyst: (a) blue line – 313 K adsorption; (b) red line – 423 K desorption; (c) pink line – 673 K desorption.



**Figure S3** Nitrogen adsorption-desorption isotherm of recycled M8 catalysts.



**Figure S4** Pore size distribution of recycled M8 catalysts.



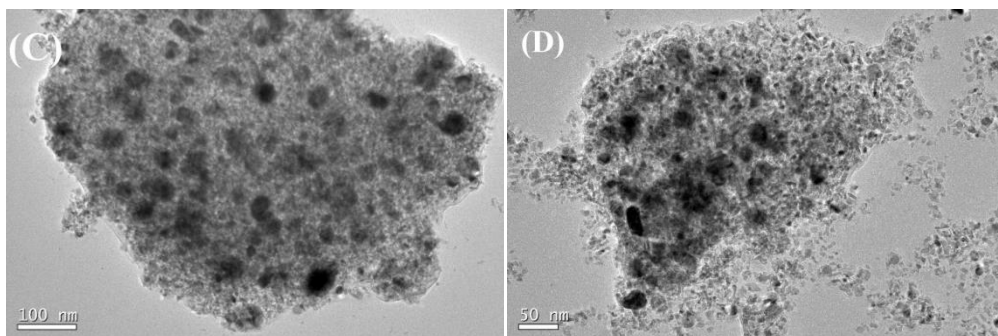


**Figure S5** HR-TEM images of M8 catalyst: (A) fresh-773 K reduction; (B) used twice without reactivation; (C) used four times without reactivation; (D) fresh-823 K reduction.

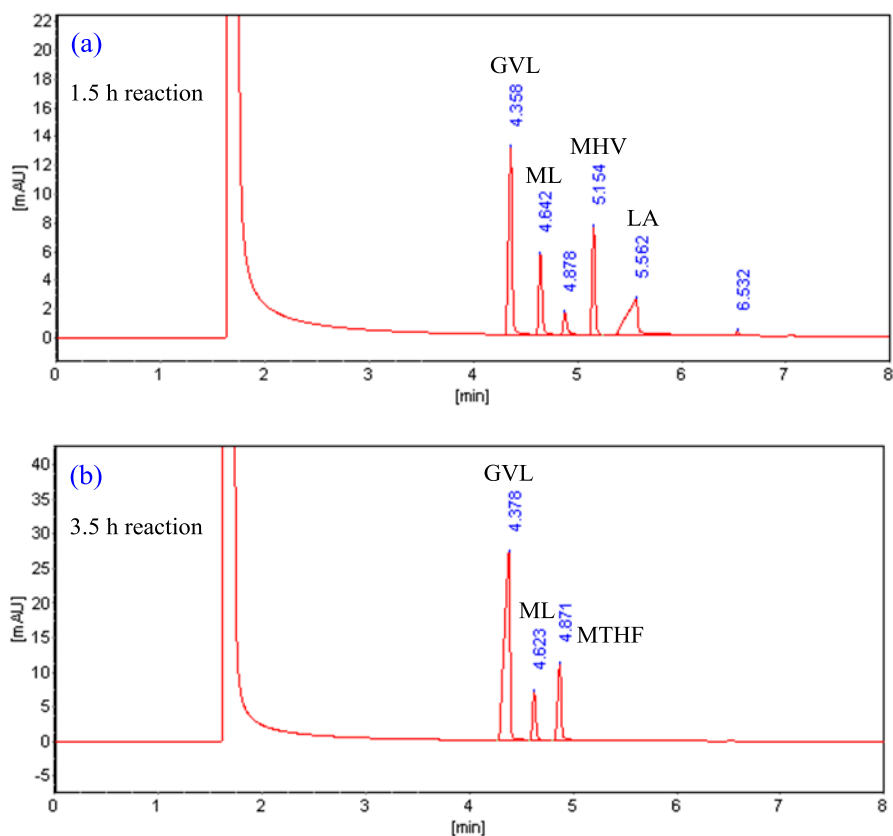


**Figure S6** GC of M8-catalyzed LA conversion into GVL. Reaction conditions: (a) LA (476 mg, 4.1 mmol), M8 catalyst (119 mg, 25 wt % relative to LA), methanol (20 mL), H<sub>2</sub> (2.0 MPa), 415 K, 1.5 h; (b) LA (476 mg, 4.1 mmol), M8 catalyst (142 mg, 30 wt % relative to LA), methanol (20 mL), H<sub>2</sub> (2.0 MPa), 415 K, 3.5 h.

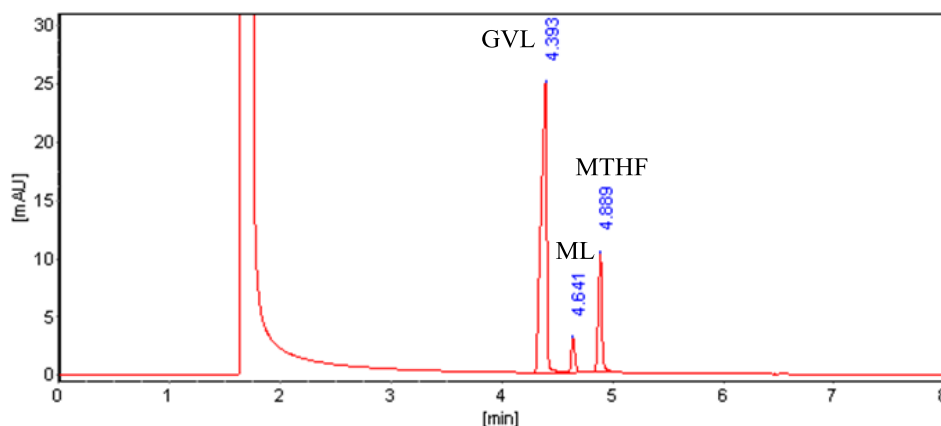


**Figure S7** GC of M8-catalyzed LA conversion into GVL. Reaction conditions: LA (476 mg, 4.1 mmol), M8 catalyst (119 mg, 25 wt % relative to LA), methanol (20 mL), H<sub>2</sub> (4.0 MPa), 415 K, 3 h.

**Table S1** ICP-AES analysis of reaction solution

Condition	<sup>c</sup> Ni, ppm	<sup>c</sup> Cu, ppm
a	0.98	0
b	2.01	0

<sup>a</sup>: catalyzed by fresh M8 catalyst; <sup>b</sup>: M8 catalyst used for the second time; <sup>c</sup>: residual Ni or Cu in reaction solution.

**Table S2** Comparison of activity among various metal catalysts

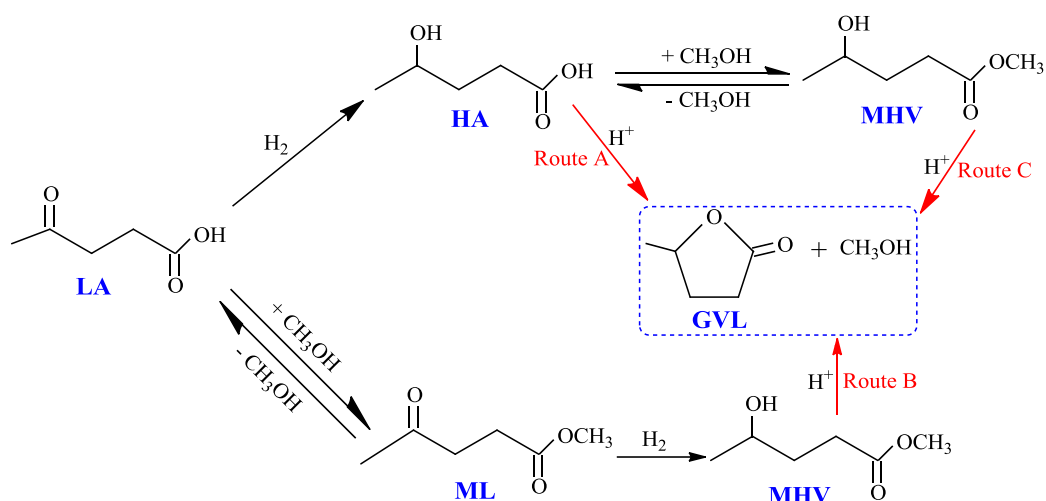
Catalysts	TOF m <sub>GVL</sub> m <sub>(active sites)</sub> <sup>-1</sup> h <sup>-1</sup>	GVL yield %	GVL selectivity %
Ru/C	26.10	97.0	97.0
<sup>a</sup> Ru/C	19.24	71.5	93.0
<sup>b</sup> Ru/C	15.36	57.1	90.3
Pd/C	3.60	12.7	60.1
Pt/C	4.42	8.5	47.5
M8	1.98	98.1	98.1

Reaction conditions: LA (476 mg, 4.1 mmol), catalysts (119 mg), methanol (20 mL), H<sub>2</sub> (2.0 MPa), 415 K, 3 h; <sup>a</sup>: Ru/C used for the second time without treatment; <sup>b</sup>: Ru/C used for the third time without treatment.

### Proposed reaction mechanism

The possible reaction pathway for the conversion of LA into GVL over M8 catalyst in methanol medium was deduced based on GC-MS analysis (Figures S8 and S9). The products were identified as HA, ML, GVL, MHV, and LA, respectively. As shown in Scheme 1, three possible reaction pathways were available for GVL production, including (A) the hydrogenation of LA into HA followed by dehydration to GVL, which was in good agreement with that reported in previous work<sup>2-5</sup>; (B) the esterification of LA with methanol into ML followed by hydrogenation into MHV, and

then further acid-catalyzed into GVL; (C) the hydrogenation of LA into HA followed by esterification with methanol to form MHV, and then further acid-catalyzed into GVL. HA, ML and MHV were detected as the intermediates that were created via hydrogenation or esterification process under the catalyzing of metal active sites and acid sites. Furthermore, the hydrogenation of intermediates HA and methyl 4-hydroxyvalerate (MHV) could be accelerated to a certain degree due to the presence of acid sites.



**Scheme 1** Possible pathway for LA hydrogenation.



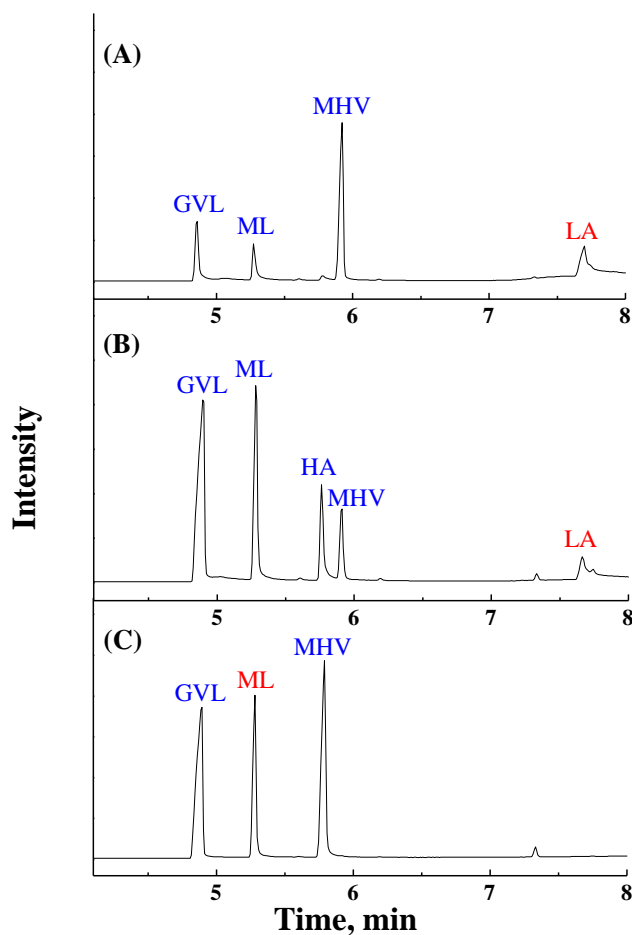


**Figure S8** GC-MS spectra of obtained samples. Reaction conditions: (A) LA (476 mg, 4.1 mmol), M8 catalyst (143 mg), methanol (20 mL), H<sub>2</sub> (2.0 MPa), 415 K, 1.5 h; (B) LA (476 mg, 4.1 mmol), M8 catalyst (119 mg), methanol (20 mL), H<sub>2</sub> (2.0 MPa), 415 K, 0.5 h; (C) ML (424 mg, 3.26 mmol), M8 catalyst (119 mg), methanol (20 mL), H<sub>2</sub> (2.0 MPa), 415 K, 3 h.

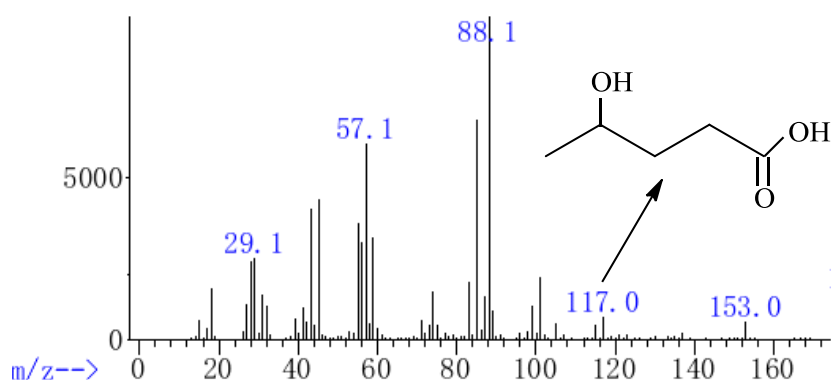


**Figure S9-1** MS of 4-hydroxyvaleric acid.

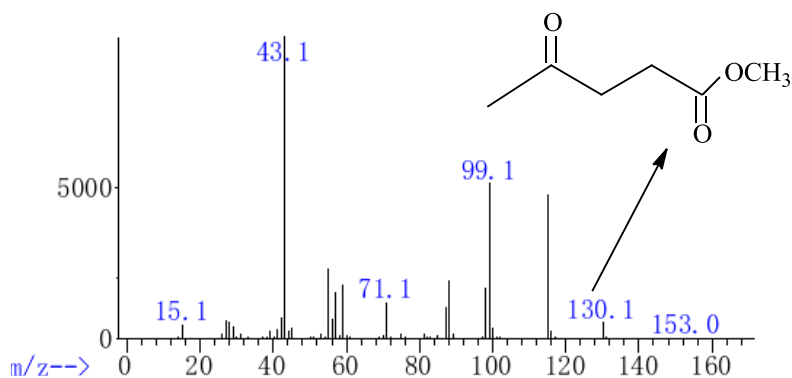


**Figure S9-2** MS of methyl levulinate.

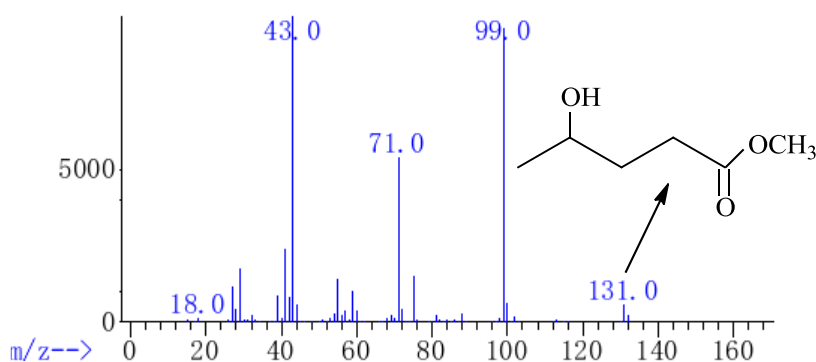


**Figure S9-3** MS of methyl 4-hydroxyvalerate.

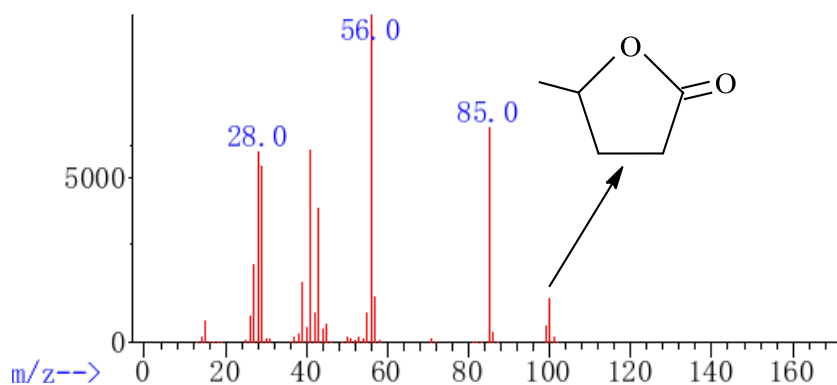


**Figure S9-4** MS of  $\gamma$ -valerolactone.

## REFERENCE

- (1) Velu, S.; Sabde, D. P.; Shah, N.; Sivasanker, S. New hydrotalcite-like anionic clays containing  $\text{Zr}^{4+}$  in the layers: synthesis and physicochemical properties. *Chem. Mater.* **1998**, *10*, 3451–3458.
- (2) Mai, E. F.; Machado, M. A.; Davies, T. E.; Lopez-Sanchez, J. A.; Da Silva, V. T. Molybdenum carbide nanoparticles within carbonnanotubes as superior catalysts for  $\gamma$ -valerolactone production via levulinic acid hydrogenation. *Green Chem.* **2014**, *16*, 4092–4097.

- (3) Yan, Z. P.; Lin, L.; Liu, S. J. Synthesis of  $\gamma$ -valerolactone by hydrogenation of biomass-derived levulinic acid over Ru/C catalyst. *Energy & Fuels* **2009**, *23*, 3853–3858.
- (4) Galleti, A. M. R.; Antonetti, G.; De Luise, V.; Martinelli, M. A sustainable process for the production of  $\gamma$ -valerolactone by hydrogenation of biomass-derived levulinic acid. *Green Chem.* **2012**, *14*, 688–694.
- (5) Wright, W. R. H.; Palkovits, R. Development of heterogeneous catalysts for the conversion of levulinic acid to  $\gamma$ -valerolactone. *ChemSusChem* **2012**, *5*, 1657–1667.